Cell

Profiling by Image Registration Reveals Common Origin of Annelid Mushroom Bodies and Vertebrate Pallium

Raju Tomer,[1,*] Alexandru S. Denes,[1,2] Kristin Tessmar-Raible,[1,3] and Detlev Arendt[1,*]
[1]Developmental Biology Unit, European Molecular Biology Laboratory, D-69117 Heidelberg, Germany
[2]Present address: Biozentrum, University of Basel, Klingelbergstrasse 50/70, CH-4056 Basel, Switzerland
[3]Present address: Max F. Perutz Laboratories, Campus Vienna Biocenter, Dr. Bohr-Gasse 9/4, A-1030 Vienna, Austria
*Correspondence: tomer@embl.de (R.T.), arendt@embl.de (D.A.)
DOI 10.1016/j.cell.2010.07.043

SUMMARY

The evolution of the highest-order human brain center, the "pallium" or "cortex," remains enigmatic. To elucidate its origins, we set out to identify related brain parts in phylogenetically distant animals, to then unravel common aspects in cellular composition and molecular architecture. Here, we compare vertebrate pallium development to that of the mushroom bodies, sensory-associative brain centers, in an annelid. Using a newly developed protocol for cellular profiling by image registration (PrImR), we obtain a high-resolution gene expression map for the developing annelid brain. Comparison to the vertebrate pallium reveals that the annelid mushroom bodies develop from similar molecular coordinates within a conserved overall molecular brain topology and that their development involves conserved patterning mechanisms and produces conserved neuron types that existed already in the protostome-deuterostome ancestors. These data indicate deep homology of pallium and mushroom bodies and date back the origin of higher brain centers to prebilaterian times.

INTRODUCTION

In human and other mammals, the pallium represents the most highly developed part of the forebrain, the site of learning and memory (Kandel et al., 2000). It harbors huge densities of interneurons arranged in cortical layers around a central neuropil (hence, "cortex"; Figure 1). The pallium is less elaborate in other vertebrates and generally thought to function as a sensory-associative center integrating primarily olfactory information (Nieuwenhuys, 2002). Insects and spiders, but also annelids, form similar brain centers with densely packed neurons that send out thousands, in some species hundreds of thousands, of approximately parallel processes that form a central, lobed neuropil (Strausfeld et al., 1998) (Figure 1). These likewise represent sensory-associative brain centers implicated in olfactory discrimination, as well as in olfactory learning and memory (Heisenberg, 2003; Strausfeld et al., 2009). Anatomical, structural, and functional similarities of the evolutionarily more ancient parts of the vertebrate pallium, the "paleopallium" and "archipallium," with, for example, mushroom bodies of neopteran insects have long been noted and interpreted as convergent acquisitions as a result of functional constraints in independent evolutionary lineages (Farris, 2005, 2008; Strausfeld et al., 1998). Also, the evolution of characteristic folds and fissures and the subpartitioning into functional units have occurred independently in the mammalian pallium and several times in insect mushroom bodies (Farris, 2008). These multiple convergences, however, do not rule out the possibility that vertebrate pallium and invertebrate mushroom bodies ultimately trace back to a common evolutionary precursor. Some less elaborate, sensory-associative brain centers may have already existed in the protostome ancestor (of, among others, insects and annelids) or even in the last common ancestor of protostomes and deuterostomes (to which vertebrates belong). These may have given rise to vertebrate pallium and invertebrate mushroom bodies alike.

We set out to decide between the two alternatives—independent evolution versus common origin of pallium and mushroom bodies from ancient sensory-associative brain centers—by the detailed molecular comparison of their development and differentiation. Previous studies revealed conserved expression of various transcription factors in vertebrate and invertebrate forebrains, but a specific comparison of gene expression in associative brain centers has not been undertaken. For this, we investigated mushroom body development in the marine annelid *Platynereis dumerilii* (Fischer and Dorresteijn, 2004), to then compare to available vertebrate data. *Platynereis* is an "errant" annelid with huge mushroom bodies (Müller, 1973) that actively explores the environment and shows some sort of learning (Evans, 1966). Fortunately, for the purpose of genetic comparison, the *Platynereis* transcriptome has proven to be "slow evolving," exhibiting less evolutionary change than that of other protostomes with mushroom bodies (*Drosophila*, *Apis*) (Raible et al., 2005). Also, in line with a slower evolutionary pace of the annelid lineage, we have shown that *Platynereis* neural patterning exhibits ancient characteristics, many of which are shared with the vertebrates but not with the faster-evolving fly

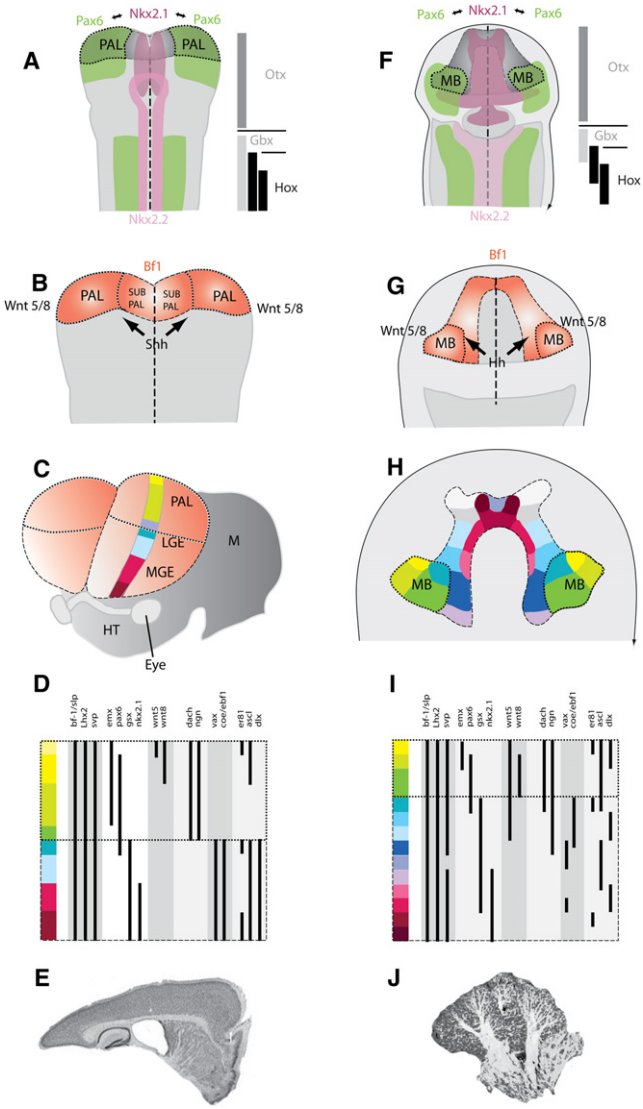

Figure 1. Comparison of Vertebrate Pallium and Annelid Mushroom Body Development Based on Previous Work and on This Study

(A–E) Development of the mouse pallium from open neural plate early specification (5 s; A and B) to E10.5 late specification stage (C and D) and adult (E).

(F–J) Development of the *Platynereis* mushroom bodies from 48 hpf specification stage (F–I) to adult (J). Note that in mouse, elaborate morphogenesis (neural tube and telencephalic vesicle formation) occurs between early and late specification stages, which does not take place in the annelid.

(A) The mouse pallium (PAL) anlage with reference to the anterior-posterior (*otx*, *gbx*, *hox*) and mediolateral (*pax6*, *nkx2.1*, *nkx2.2*) regional patterning systems. (After Inoue et al. [2000] and Shimamura et al. [1995].)

(B) Expression of *bf-1* (orange) outlining the telencephalon anlage including the pallium. Wnt5/8 and Shh indicate spatially restricted activity of signaling ligands implicated in telencephalon development.

(C) Regionalization of telencephalic vesicles into pallium (PAL) and lateral and medial ganglionic eminences (LGE, MGE). Colored strip indicates level of cross-section in (D). M, mesencephalon; HT, hypothalamus, Eye, position of cutoff eye stalk.

(D) Gene expression along the telencephalic section in (C) indicated by black bars and color code. For references, see the main text.

(E) Parasagittal section of the mouse cortex.

(F) The *Platynereis* mushroom body anlage with reference to the anterior-posterior (*otx*, *gbx*, *hox*) and mediolateral (*pax6*, *nkx2.1*, *nkx2.2*) regional patterning systems. MB, mushroom bodies.

(G) Expression of *bf-1* (orange) in the annelid brain at 48 hpf. Wnt5/8 and Hh indicate spatially restricted expression of conserved ligands.

(H) Brain molecular topography of the *bf-1*+ region at 48 hpf as revealed by this study. Color code refers to (I).

(I) Gene expression in the *Platynereis* brain indicated by black bars and color code referring to (H).

(J) The *Platynereis* adult mushroom bodies, parasagittal section.

See also Figure S2.

and nematode lineages (Denes et al., 2007; Tessmar-Raible et al., 2007). Finally, *Platynereis* is easy to breed and thus accessible to high-throughput approaches (Fischer and Dorresteijn, 2004), as a prerequisite for the analysis of multiple genes.

Previous comparisons of brain development between phylogenetically remote species have been restricted to gene-by-gene comparisons that did not allow, or allowed only in a coarse manner, relating expression data spatially for multiple genes. To overcome this, we have established a new protocol for Profiling by Image Registration (PrImR) that, for the first time, allows alignment of expression images with cellular resolution and thus expression profiling for the whole brain at the single-cell level. Our protocol builds on the highly stereotypical nature of *Platynereis* neurodevelopment to align expression patterns for an unlimited number of genes in an additive process.

Using PrImR, we first investigated whether the overall molecular topography of the brain anlage is conserved between annelid and vertebrate and whether the *Platynereis* mushroom bodies develop from corresponding molecular regions when compared to vertebrate pallium (as a test for homology) (Arendt, 2005; Woodger, 1945). We also tested whether the positioning of both follows similar developmental patterning mechanisms. Next, we used PrImR to determine the expression profile for specific subregions, focusing on specifically expressed genes making up the regulatory and differentiation signature of cells developing from these regions and compared this "molecular fingerprint" (Arendt, 2008) to that of vertebrate telencephalic neuron types but also to that of the mushroom body neuroblasts in *Drosophila*. We conclude that pallium and mushroom body most likely evolved from the same (sensory associative) brain center that was already present in the bilaterian ancestors.

RESULTS

In Silico Alignment of Gene Expression Patterns

To establish a high-resolution molecular topography of the annelid brain and to investigate the molecular fingerprint of brain subregions, we set out to obtain coexpression information for a large number of specifically expressed genes. This is impossible to achieve at large scale by two-color double whole-mount in situ hybridization (Tessmar-Raible et al., 2005), because this would require a nonlinearly increasing amount of technically demanding experiments. To overcome this, we took advantage of the observation that *Platynereis* development is highly stereotypic and synchronous within and across batches (Fischer and Dorresteijn, 2004) and developed a computational protocol for

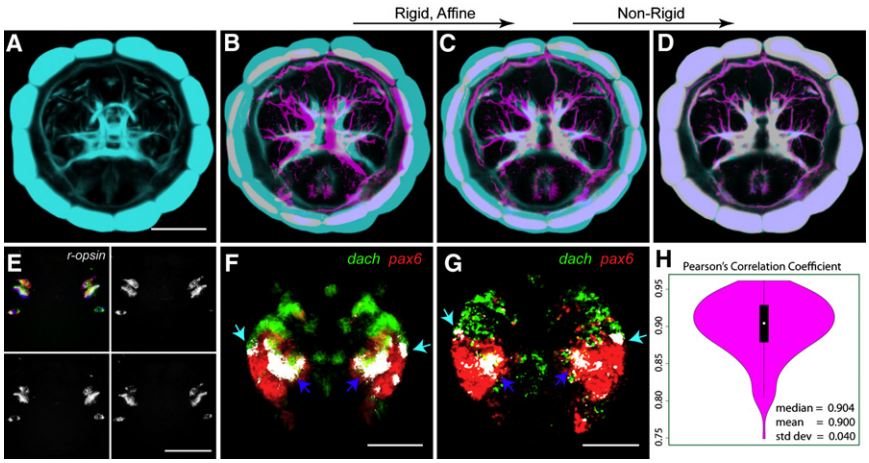

Figure 2. In Silico Alignment of Expression Patterns

(A) Maximum Z projection of average reference axonal scaffold image of 48 hpf larval brain.

(B–D) Step-wise alignment of an axonal scaffold image to the average reference scaffold (cyan) using rigid, affine, and smoothened freeform nonrigid transformations. Images are 20 μm thick optical sections. See Movies S1 and S2 for details.

(E) A positive control experiment to test the accuracy of the alignment algorithm. All images are maximum Z projections of aligned expression patterns of r-opsin, acquired from three different larvae, and an RGB merge of them. See Movie S3 for details.

(F and G) Experimental validation of an in silico coexpression (F) using double fluorescence WMISH double staining (G). White, colocalization of green and red pixels. Cyan and blue arrows point to verified coexpression.

(H) Violin plot illustrating the distribution of Pearson's correlation coefficients of 171 gene expression images with their gene-specific average images. Magenta shows the data density. Mean = 0.900, median = 0.904, standard deviation = 0.040.

Scale bars represent 50 μm. See also Figure S1 and Movies S1, S2, and S3.

accurately aligning the expression patterns of different genes acquired from different stained individuals of identical developmental stage (Profiling by Image Registration, PrImR, |•primər|). In the first step, two-channel image stacks were acquired via whole-mount reflection confocal laser-scanning microscopy (Jékely and Arendt, 2007). One channel contained information on the expression pattern of a given gene and the other on the axonal scaffold of the *Platynereis* larval brain. More than three biological replicas were acquired for every gene. Next, we used the axonal scaffold channel to align these images to a reference average axonal scaffold image (Figure 2A, Figure S1 available online), first via rigid alignment algorithms and then by smooth nonrigid transformation (see the Experimental Procedures) (Figures 2B–2D). For each gene, a normalized average expression image from (in most cases) five individuals was thus generated (Figure S1B) that was directly comparable to those of an unlimited number of other genes. As a test for accuracy, we obtained almost perfect overlap of signal for single cells stained for the same gene in different individuals (Figure 2E). We also found that the coexpression images obtained by our PrImR protocol fully reproduced those obtained by double-fluorescent WMISH (Tessmar-Raible et al., 2005) (compare Figures 2F and 2G) but tended to be more "complete," reflecting the higher sensitivity of the NBT/BCIP staining and of the reflection microscopy technique (Jékely and Arendt, 2007). Finally, to challenge the accuracy of the protocol, we systematically estimated the extent of overlap between individually aligned scans by calculating the Pearson's correlation coefficient for 171 individually aligned scans with the gene-specific average image (see the Experimental Procedures) and found that the probability is highest to obtain a value above 0.9, which implies that the average expression images used for this study should reliably reproduce endogenous gene expression. Our protocol thus allows the comparison of any newly added expression pattern to all preexisting patterns at once, with high accuracy and in cellular resolution.

The Molecular Topography of the *Platynereis* Brain

We used our PrImR protocol to determine the molecular topography of the *Platynereis* brain after 2 days of development, to test whether any of the *Platynereis* forebrain regions would show "telencephalon-like" coordinates. At this stage, major subregions of the developing *Platynereis* nervous system are already established and larger populations of neurons have started differentiation (Tessmar-Raible et al., 2007). For our purposes, it was sufficient to focus on one stage only, because in the absence of drastic morphogenetic changes (such as neurulation and vesicle formation in vertebrates), gene expression patterns in the developing *Platynereis* brain remain spatially constant over time (as shown for example for *pax6, six1/2* [Arendt et al., 2002] or *dach* and *bf-1* [Figures 5 and 6]), indicating colocalization and temporal co-occurrence of differentiated neurons and their precursors.

We had previously shown that both the annelid and vertebrate brains exhibit a basic subdivision into medial *nk2.1*+ and lateral *pax6*+ subregions (Tessmar-Raible et al., 2007) (Figure 1A) (transformed into a ventral-dorsal arrangement during vertebrate neurulation; Figures 1A–1C). It is within this conserved framework that the vertebrate telencephalon anlage is established, with the pallium developing from the anterior part of the *pax6*+ region (Figure 1A). The outline of the whole telencephalon anlage is demarcated early on by expression of *bf-1* (Hébert and Fishell, 2008) (orange in Figure 1B), a crucial regulator of telencephalic development (Danesin et al., 2009). In the course of telencephalic morphogenesis, *gsx*+ and *emx*+ (Kimura et al., 2005) domains complement the *nk2.1*+ and *pax6*+ subregions (Figures 1C and 1D) such that the *gsx*+, *pax6*+ overlap demarcates the future pallial-subpallial boundary (Danesin et al., 2009; Yun et al., 2001) and *pax6*+, *emx*+ coexpression specifies pallial telencephalic precursors (Kimura et al., 2005). Besides *bf-1*, *lhx2* (expressed broadly in the telencephalon and acting highly up in the hierarchy of cortical induction (Hébert and Fishell, 2008), *COUP-TF1/seven-up* (contributing to telencephalic

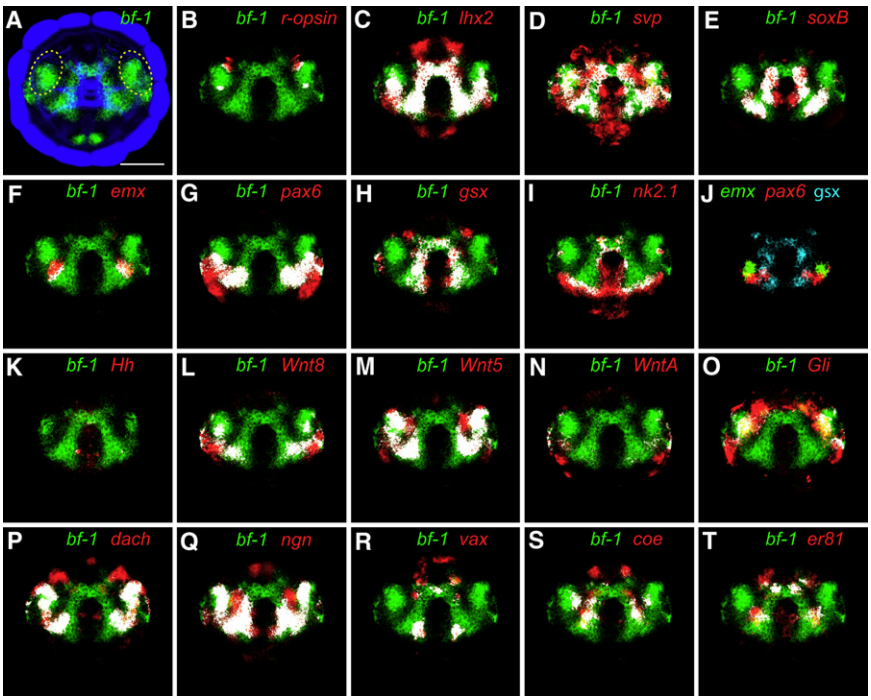

Figure 3. Coexpression of "Telencephalic" and Other Marker Genes, Red, with *bf-1*, Green, in the *Platynereis* 48 hpf Larval Brain

(A and B) Complete expression of *bf-1* (green) (A). Blue, reference axonal scaffold. Dotted circle marks expression in the eye field, as indicated by *r-opsin* coexpression in (B).

(C–E) genes covering the almost entire *bf-1* domain.

(F–I) Lateral-to-medial sequence of regionalisation genes.

(J) Five-micron-thick optical section showing lateral-to-medial coexpression of *emx* (green), *pax6*(red), and *gsx* (cyan).

(K–O) Genes involved in mediolateral signaling.

(P–T) Genes showing mediolaterally restricted expression.

All images are Maximum Z projections of slice numbers 13 to 40, i.e., 28 μm thick (except K: 8–28, i.e., 21 μm thick) in the reference scaffold image stack. White marks colocalizing pixels. Scale bars represent 50 μm. See also Figure S5.

patterning (Hébert and Fishell, 2008) and soxB family members (*sox1*[Ekonomou et al., 2005] and *sox2* [Bani-Yaghoub et al., 2006]) play important roles in early telencephalic development (Figure 3E), although the spatial distribution and coexpression of these factors along the anterior-posterior and mediolateral brain axes is not fully resolved for the vertebrates.

We accordingly examined *bf-1, lhx2*, *svp*, *soxB*, *pax6*, *emx*, *gsx*, and *nk2.1* expression in *Platynereis* and indeed identified a brain region with telencephalon-like molecular topography (Figures 3A–3I; summarized in Figure 1). First, we found *bf-1* expressed in a horseshoe-shaped domain in the *Platynereis* brain (Figure 3A), where it is specifically coexpressed with *lhx2*, *svp*, and *soxB* (Figures 3C–3E). (The more lateral part of *bf-1*+ domain represents the eye anlage; Figure 3B.) Second, from lateral to medial, the *Platynereis bf-1* brain domain is subdivided by spatially restricted coexpression of *emx*, *pax6*, *gsx*, and *nk2.1* (Figures 3F–3J) in a telencephalon-like fashion. Nowhere else in the developing *Platynereis* larva was a similar sequence of *emx*+/*pax6*+, *pax6*+, *pax6*+/*gsx*+, *gsx*+, and *gsx*+/*nk2.1*+ subregions (Figure 3J) detected. The *emx*+/*pax6*+ and *pax6*+ regions within the *bf1*+ domain thus represented candidate counterpart regions to the vertebrate pallium anlage, a notion that we decided to explore further.

Comparison of Patterning Mechanisms

In vertebrates, bf-1 coordinates the activity of two opposing signaling centers that pattern the telencephalon anlage. bf-1 acts downstream of the ventral signal, Hh, to induce ventral (subpallial) identities. At the same time, bf-1 inhibits dorsal Wnt/β-catenin signaling through direct transcriptional repression of *Wnt8* (Danesin et al., 2009), which induces dorsal (pallial) identities (Houart et al., 2002). Vertebrate telencephalic patterning can be perturbed by ectopic β-catenin activation (mimicking the dorsal signal), which accordingly triggers the upregulation of dorsal pallial and downregulation of ventral subpallial markers (Backman et al., 2005). Investigating the expression of orthologous signals and factors in *Platynereis*, we indeed detected *Hh* in the medial (Figure 3K) and *Wnt8* in the lateral brain (Figure 3L), matching the vertebrate situation. We also observed lateral expression of *Wnt5* (Figure 3M), another dorsal Wnt signal implicated in corticospinal axon guidance (Keeble et al., 2006), of *WntA* (not found in vertebrates; Figure 3N) and *Gli* (Figure 3O), a zinc finger transcription factor essential for dorsal telencephalic fates (Tole et al., 2000). None of the other *Platynereis* Wnt genes was expressed in the brain (data not shown; note that *Wnt3* does not exist in annelids). For *Platynereis*, exposure to the chemical compound 1-Azakenpaullone has been established as an efficient means to ectopically induce β-catenin activation (Schneider and Bowerman, 2007). We accordingly tested the effect of 1-Azakenpaullone on *Platynereis* brain regionalization and observed upregulation of lateral *emx* expression (Figures 4B and 4G), downregulation of intermediate *gsx* (Figures 4D and 4I), and medial *nk2.1* expression (Figures 4E and 4J), while *pax6* appeared unaffected (Figures 4C and 4H). These results mirror vertebrate telencephalic patterning (Figure 1) and are thus strongly indicative of evolutionary conservation.

The Molecular Fingerprint of Mushroom Body Neurons

In vertebrates, distinct combinations of differentially expressed transcription factors control the fate of the various telencephalic subregions. We took advantage of PrImR to further determine and compare molecular fingerprints. In mouse, dorsal telencephalic (pallial) *pax6*+ regions show differential activity of Dach (Caubit et al., 1999) and ngn1/2, bHLH factors required for pallial

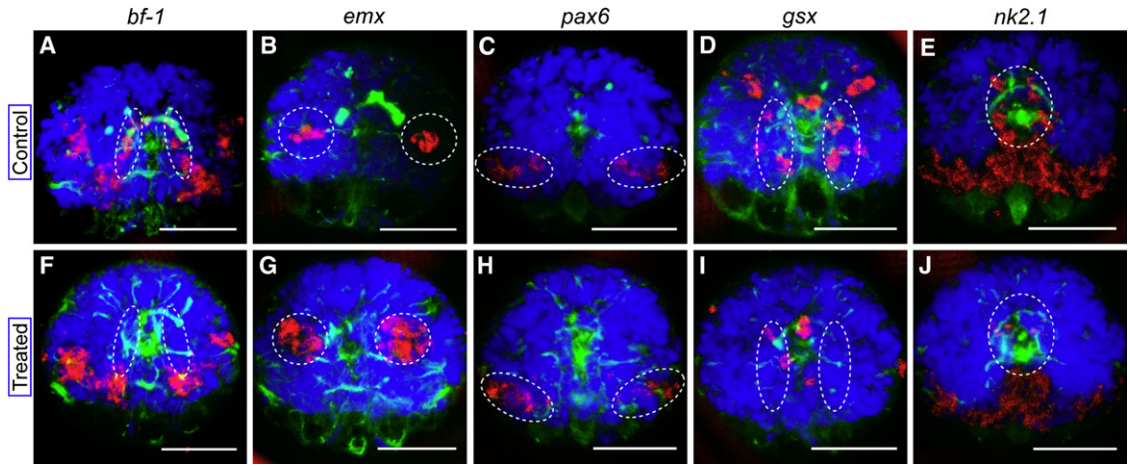

Figure 4. Differential Gene Regulation in the Developing *Platynereis* Brain

Expression of *bf-1*, *emx*, *pax6*, *gsx*, and *nk2.1* in DMSO control (A–E) and 1-Azakenpaullone (1 μM final concentration) treated 48 hpf larval brain (F–J). Changes in expression patterns are highlighted by dashed circles. Blue, nuclear stain DAPI; green, immunostaining against acetylated tubulin. n for *bf-1*: treated > 200, control > 200; *emx*: treated > 380, control > 300; *pax6*: treated > 350, control > 310; *gsx*: treated > 150, control > 160; *nk2.1*: treated > 320, control > 200. Scale bars represent 50 μm.

neurogenesis (Nieto et al., 2001). In *Platynereis*, *dach* and *ngn* are similarly restricted to *emx*+, *pax6*+ subregions (Figures 3P and 3Q; compare Figures 1D and 1I). In mouse, ventral (subpallial) *gsx*+ regions coexpress *vax1*, required for GABAergic interneuron generation (Taglialatela et al., 2004), and coe/ebf1, an HLH transcription factor affecting subpallial development (Garel et al., 1999). We accordingly found both genes coexpressed in *Platynereis gsx*+ regions (Figures 3R and 3S; compare Figures 1D and 1I). In mouse, telencephalic subregions express er81, an ETS factor active in distinct subpallial domains (Yun et al., 2001) and direct target of pax6 in the dorsal pallium (Tuoc and Stoykova, 2008). *Platynereis er81* is similarly expressed in the *pax6*+/*gsx*+ and *gsx*+/*nk2.1*+ subregions but not in between (Figure 3T; compare Figures 1D and 1I). Adding to this, expression of *Platynereis* genes orthologous to *ascl1/mash1* (bHLH downstream effector of gsx1 [Wang et al., 2009]; expressed in ventral and dorsal telencephalon [Yun et al., 2001]), to *brn1/2/4* (POU domain transcription factors required for cortical migration in dorsal and ventral telencephalon [Ekonomou et al., 2005; McEvilly et al., 2002]), and to many other genes implicated in telencephalon development by function or by expression is detailed for *Platynereis* in Figure S2 and has been used to generate the molecular map in Figure 1H. The overall comparison suggests that the molecular fingerprints of annelid and vertebrate *emx*+/*pax6*+, *pax6*+, *pax6*+/*gsx*+, *gsx*+, and *gsx*+/*nk2.1*+ subregions are similar to large extent but may also differ in the detail (for example, *dlx* is expressed more broadly in annelid than in vertebrate; *rx* is expressed in the *emx*+, *pax6*+, and *gsx*+ subregions in the annelid but excluded in the vertebrate; Figure S2).

Positioning the *Platynereis* Mushroom Body Anlagen

Since our molecular comparison had identified one unique candidate region in the *Platynereis* brain, which, by position, similar responsiveness to Wnt signaling, and similar molecular fingerprint (*bf1*+, *emx*+, *pax6*+, *dach*+, *svp*+, *tll*+, *ngn*+, *asc*+) qualified as possible evolutionary counterpart to the vertebrate pallium anlage (encircled by stippled line in Figures 1C and 1D), we set out to determine whether this paired region indeed represented the *Platynereis* mushroom body anlagen by tracing mushroom body development from adult (Figure 5, Figure S3, Movie S4) and juvenile stages (10 days postfertilization [dpf], when they are fully developed and can be easily identified histologically) back to earlier larval stages. We combined anatomical (the specific shape of mushroom bodies), histological (the dense packing of neurons), and topological (the specific spatial arrangement of mushroom bodies and palpal and antennal nerves) evidence, as well as the expression of mushroom body-specific marker genes (*dach* and *pax6*), to reidentify and position the developing mushroom bodies at various stages (6 weeks, 20, 10, 9, 8, 7, 6, 5, 4, 3, and 2 dpf; Figure 5 and data not shown). This allowed unambiguous positioning of the mushroom body anlagen to ventrolateral coordinates at 48 hr postfertilization [hpf] that indeed matched the *emx*+, *pax6*+, *dach*+ candidate region.

In juvenile worms, the differentiating *emx*+, *pax6*+ mushroom bodies and the more medial *gsx*+, *nk2.1*+ brain tissue (referred to as "pars intercerebralis"[Müller, 1973]) continued to express *bf-1* (Figure 6A) and started to specifically express *arx* (Figure 6B; expressed in mouse and fish telencephalon and ventral thalamus [Miura et al., 1997]). We also detected specific expression of two conserved bilaterian microRNAs, *miR-9* and *mir-9** (Christodoulou et al., 2010) (Figures 6C and 6D). In the vertebrates, these microRNAs are expressed only in the telencephalon, among all differentiated CNS tissues (Deo et al., 2006). Regarding transmitter usage, large part of the *Platynereis* mushroom bodies proved glutamatergic by expression of *vglut*, encoding the vesicular glutamate transporter (Figure 6F). In contrast, *gad*, a marker for GABAergic neurons, was restricted to more medial brain tissue (Figure 6E), as was the dopaminergic

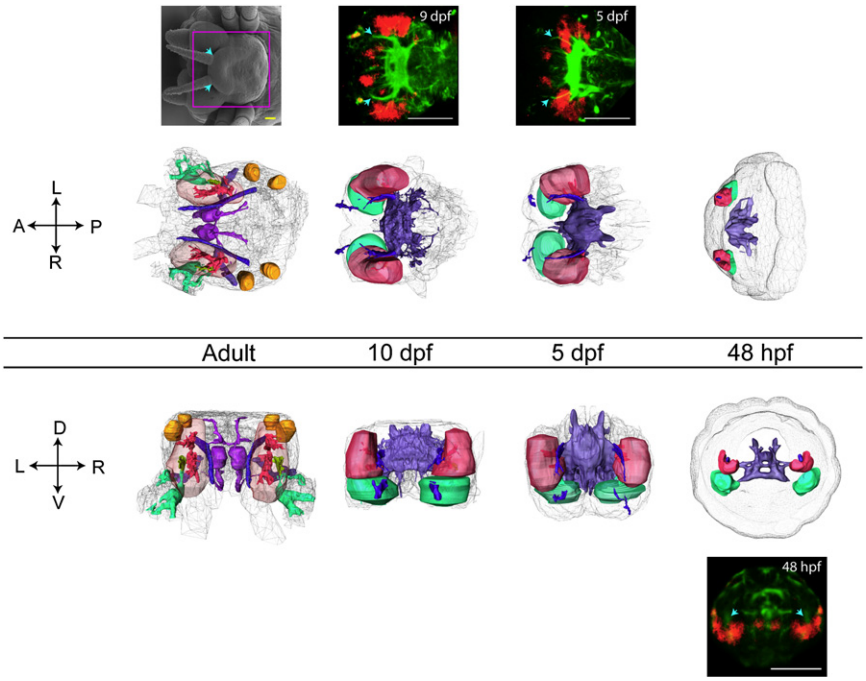

Figure 5. *Platynereis* Mushroom Body Development

Three-dimensional models were generated for various stages according to confocal image stacks (see Movie S4 for details). Depicted structures represent mushroom body pedunculi (red), mushroom body perikarya (transparent red), antennal nerve (dark blue), pars intercerebralis (purple), eyes (yellow), palpae (green), and a glomerulus-like structure (mediates the connection between palpae and mushroom bodies; light green). Continuous expression of *dach* (top and bottow row) in mushroom body neurons consistent with anatomical backtracing. Blue arrows point to the antennal nerve. A, P, D, V, L, and R indicate body axes.

Scale bars represent 50 μm. See also Figure S3 and Movie S4.

marker *tyrosine hydroxylase* (Figure 6H), again matching the vertebrate situation (Marín and Rubenstein, 2001). However, we also detected a difference in the spatial distribution of transmitter type in that *Platynereis* mushroom bodies also harbored cholinergic neurons (Figure 6G; not found in the vertebrate pallium).

Molecular Fingerprint Comparison with Insect Mushroom Bodies

Mushroom bodies of similar cellular composition also exist in arthropods such as onychophorans (velvet worms), spiders, and insects, yet ample molecular data exist only for the mushroom bodies in insects. In *Drosophila*, mushroom body neuroblasts require *pax6* and *dach* for their specification but do not express *sine oculis* (*six1/2*) or *eyes absent* (*eya*) (Noveen et al., 2000). We found that the only region of the *Platynereis* brain coexpressing *pax6* and *dach* but devoid of *six1/2* and *eya* is indeed the mushroom body anlage (Figures 7A and 7B and *eya* data not shown), indicative of evolutionary conservation. To challenge homology of insect and annelid mushroom bodies, we looked for a combination of transcription factors that, by coexpression, uniquely define *Drosophila* mushroom body neuroblasts independent of pax6 and dach—to then test whether a similar coexpression would locate to the annelid mushroom body anlage in an equally specific manner. Among the four *Drosophila* mushroom body neuroblasts, Pcd8 andPcd9 are uniquely identified by the specific coexpression of *asc/l'sc*, *tll*, *svp*, *slp/bf-1*, and *otx* (Urbach and Technau, 2003). We determined by PrImR where in the *Platynereis* 48 hpf brain these five transcription factors would be coexpressed, and indeed the only two bilateral spots of cells in the *Platynereis* brain coexpressing them form part of the mushroom body anlage (Figures 7C–7H). This is strong evidence in favor of an evolutionary relatedness of insect and annelid mushroom bodies. However, in contrast to annelid mushroom bodies (Figure 7I) and to vertebrate pallium, the *Drosophila dac*+ mushroom body precursors do not express *emx*, and the overall molecular topography is conserved to lesser extent between fly, annelid, and vertebrate (Urbach and Technau, 2003) than between annelid and vertebrate. Our data suggest that this is

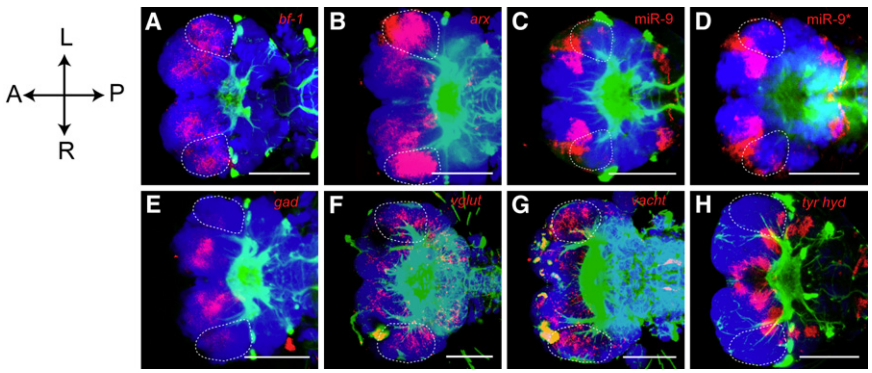

Figure 6. Gene Expression in the Brain of *Platynereis* Juvenile Worms

Transcription factors (A and B), microRNAs (C and D) and marker genes (E–H) for GABAergic (*gad*, E), glutamatergic (*vglut*, F), cholinergic (*vacht*, G), and dopaminergic (*tyrosine hydroxylase*, H) neurons. Dashed circles outline mushroom bodies. A, P, L, and R indicate body axes. Scale bars represent 50 μm.

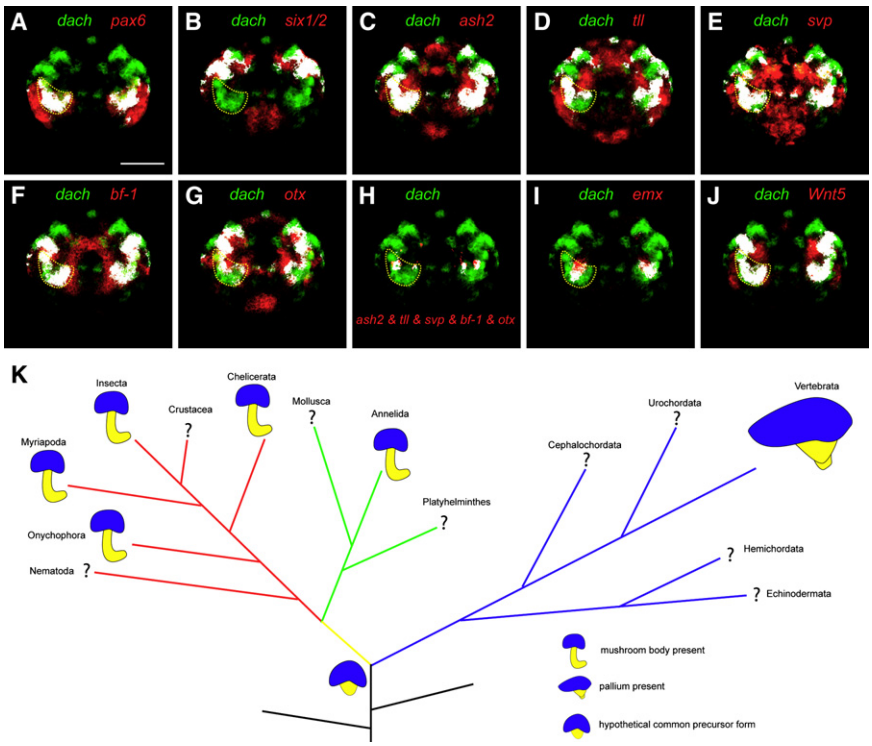

Figure 7. Coexpression of Insect Neuroblast Marker Genes, Red, with *Dach*, Green, in the *Platynereis* 48 hpf Larval Brain

(A–J) Coexpression of *dach* (green) with *pax6* (A), *six1/2* (B), *ash2* (C), *tll* (D), *svp* (E), *bf-1/slp* (F), *otx* (G), the intersection of *ash2*, *tll*, *svp*, *bf-1/slp*, and *otx* (H), *emx* (I), and *Wnt5* (J) (red). The intersection of expression patterns was generated from expression masks generated by smoothening images with a Gaussian sigma of 2 and a signal cutoff of 35. All images are Maximum Z projection of slice numbers 13 to 40, i.e., 28 μm thick, in the reference scaffold image stack. White marks colocalizing pixels.

(K) Phylogenetic distribution of mushroom body and pallium in Bilateria.

Scale bars represent 50 μm. See also Figure S4.

due to secondary modifications of mushroom body development in the insect lineage.

DISCUSSION

In this study, we have established a new protocol, PrImR, that allows expression profiling by image registration with cellular resolution for the entire organism. Expression profiling at single-cell resolution has been reported previously (Liu et al., 2009; Sugino et al., 2006), but our protocol is the first to allow simultaneous profiling for the whole central nervous system, where cells are densely packed. Our protocol thus sets the stage for a new chapter of evolutionary developmental research that has so far been restricted to gene-by-gene comparisons of expression patterns with restricted coexpression information, necessarily remaining fragmentary and sometimes inconclusive. Instead, PrImR allows much broader comparisons, involving hundreds of transcription factors and differentiation genes, and a much higher level of integration. For the first time, molecular fingerprinting as introduced here allows testing homology hypotheses such as the comparison of mushroom bodies between annelids and insects and of mushroom bodies with vertebrate pallium (Strausfeld et al., 1998) that could not be resolved on merely anatomical and physiological grounds.

Taking advantage of this new protocol, our data reveal that mushroom bodies in annelid and vertebrate pallium develop from the same, molecularly defined, subregion (*emx+/pax6+*) at similar anterior-posterior and mediolateral coordinates within an overall conserved molecular topography of the brain (Figures 1A and 1F), which is established by similar patterning mechanisms (Figures 1B and 1G). They express similar and unique combinations of additional transcription factors (*dach+*, *svp+*, *slp+*, *tll+*, *ngn+*, *asc+*, *arx+)* (Figures 1C, 1D, 1H, 1I, and 6). They give rise to glutamatergic neurons, while GABAergic and dopaminergic neuron types emerge from more medial/ventral brain regions. They are positive for the same brain-specific microRNAs (mir-9, -9*). We are confident that these similarities are too complex to be plausibly explained by independent (convergent) evolution. Instead, we propose that they were in place already in the protostome-deuterostome ancestor, the last common ancestor of annelids and vertebrates (Figure 7K).

To assess the statistical significance of our dataset, we conducted permutation tests by randomly assigning gene expression to "pallium" or "mushroom body," and we found the observed similarity in molecular fingerprint extremely unlikely to arise by chance (Figure S4; p value less than 2.0E-05). It should be stressed, however, that this value might slightly overestimate the significance of our comparison, because a subset of the involved genes may be coregulated and should be treated as a single observation.

Importantly, however, annelid mushroom body and vertebrate pallium development and specification also differ to considerable extent, which is plausible given ~600 million years of independent evolution. First, vertebrate pallium development involves neurulation and telencephalic vesicle formation (Figures 1B and 1C), which does not occur in the annelid. Second, important differences are apparent in some expression domains. For example, annelid *nk2.1* expression exhibits lateral "wings" (Figure 1F), where it overlaps with the lateral *pax6* domain (careful 3D analysis, however, reveals that this overlap is outside of the *bf1+* mushroom body anlage). Also, the developing annelid mushroom body is positive for the *rx* gene (Figure S2), which is excluded from the vertebrate telencephalon anlage (Stigloher et al., 2006). Finally, some genes are absent in the other species. For example, *Wnt3*, expressed in the dorsomedial pallium anlage, does not exist in annelids, and *WntA*, demarcating the lateral mushroom body anlage (Figure 3N), is not found in the vertebrate genomes.

What is the significance of these findings for our understanding of mushroom body and pallium/telencephalon evolution? We can infer that the last common ancestor of protostomes and deuterostomes (and thus, of annelids and vertebrates) already possessed distinct brain centers that later gave rise to the pallium in the vertebrate and to mushroom bodies in the annelid (and arthropod) lineage (Figure 7K). Based on our data, it is likely that these centers harbored subsets of glutamatergic neurons that presumably functioned in some sort of integration of sensory signals. Input was most likely chemosensory, as deduced from the primarily chemosensory input of pallium and mushroom bodies alike, in insects, spiders, and onychophorans, as well as in annelids (Strausfeld et al., 2006). (The *Platynereis* mushroom bodies receive connections from the chemosensory palpae [Movie S4].) Notably, however, the sensory input of arthropod mushroom bodies is received by distinct olfactory appendages (Strausfeld et al., 2006) and can even be visual (in spiders, honeybee and cockroach [Strausfeld and Barth, 1993]), indicating some plasticity in mushroom body connectivity. Apparently, the sensory input into sensory associative centers can change according to the needs of changing ecological niches.

We can speculate that the first function of these chemosensory integrative brain centers was to distinguish between food and nonfood, to decide about directed locomotion toward identified food sources, and, ultimately, to integrate previous experiences into some sort of "learning" (Evans, 1966). Extrapolating from the similar motor output of today's pallium and mushroom bodies, we can assume that these integrative centers already produced coordinated locomotion of some sort (Farris, 2005).

There is a long-standing notion that the vertebrate pallium comprises distinct parts of different evolutionary age, paleo-, archi-, and neopallium. Roughly, the paleopallium corresponds to olfactory cortex and the archipallium to the hippocampus, and the neopallium comprises the remainder of the cerebral hemispheres (Swanson, 2000). Paleo- and archipallium are found in all vertebrates, while the neopallium is restricted to amniotes. In line with this concept, the cellular organization of the more ancient archi- and paleopallium strikingly resembles that of annelid and arthropod mushroom bodies, in that densely packed, basophilic somata send out parallel processes intersected by afferent and efferent networks (Strausfeld et al., 1998). Intriguingly, when compared to neopallium, the hippocampus and dentate gyrus each consist of only one layer of principle neurons (Förster et al., 2006). This contrasts with the six-layered architecture of the neopallium but rather resembles the simple architecture of the mushroom bodies. We propose that such simple architecture, ancient for vertebrates, might have been in place in the urbilaterian mushroom body/pallium sensory-associative precursor structure.

As mentioned in the introduction, it is unlikely that a mushroom body-like shape was already in place in the protostome-deuterostome ancestor. Rather, it seems plausible that the common evolutionary precursor structure of mushroom bodies and pallium was morphologically less complex and that higher degrees of histological (and thus, functional) complexity were acquired independently in divergent evolutionary lineages, as repeatedly proposed (Farris, 2005, 2008; Strausfeld et al., 1998; Strausfeld et al., 2009). To settle this issue, it will be rewarding to identify brain regions with similar molecular coordinates and fingerprint in species lacking overt mushroom body morphology such as crustaceans or mollusks on the protostome side or amphioxus on the deuterostome side (Figure 7K) and to investigate possible sensory input, integrative function and locomotor output of the corresponding brain parts. If, on one hand, such less complex, "mushroom body-related" brain parts indeed exist, they will help defining a minimum set of anatomical and physiological characteristics associated with the conserved molecular fingerprints described here. This way, we would gain more insight into anatomy and function of an ancient sensory-integrative center present in the protostome-deuterostome ancestor. If, on the other, such regions do not exist, we can infer secondary loss of brain complexity. Possible evolutionary scenarios leading to reduced brain complexity include the transition to sessile or hemisessile lifestyle with filter feeding, to interstitial burrowing with minute body size, or to parasitism.

Once a better and more complete picture of mushroom body-related brain parts in bilaterians is obtained, this will set the stage for a more comprehensive view on the evolution of insect and annelid mushroom bodies and vertebrate pallium alike. What do these groups have in common that is not found in bilaterians in which mushroom body-related brain parts are present but less elaborate? This will ultimately help to link mushroom body/pallium evolution to changes in life style, locomotion, or food capture.

EXPERIMENTAL PROCEDURES

Imaging Gene Expression Patterns

We used whole-mount reflection confocal microscopy (Jékely and Arendt, 2007) to acquire gene expression pattern images. Typically, an oil immersion 40× objective on the Leica TCS SPE Confocal Microscope was used.

Alignment of Expression Patterns

For achieving highly accurate alignments of axonal scaffolds, we developed a multistep multiresolution image registration algorithm using Mutual Information (Viola and Wells, 1995) as the image similarity metric. In the first step, images were transformed rigidly with six degrees of freedom (three for translation and three for rotation) to roughly align the images. In the second step, affine transformation with 12 degrees of freedom (three for rotation, three for translation, three for scaling, and three for shear) was used to compensate for the shrinking and shearing artifacts introduced by in situ hybridization and imaging procedures. In the last step, we used a uniform grid of control points to model freeform nonrigid local deformations and used third-order B-splines to smoothly interpolate the transformations. For the affine and nonrigid registration steps, we used a multiresolution approach in which 3D images were smoothened and downsampled to various degrees before the alignment.

Average Reference Axonal Scaffold

We generated an average *Platynereis* larval axonal scaffold using images acquired from 36 different individual 48 hpf larvae (Figure S1), which was used as reference for all the alignments.

Averaging Expression Patterns

For direct comparison of the spatial expression patterns of different genes, we generated normalized average expression patterns from three or more individual larvae (see Movie S3 and Figure S1B for examples). We used

"Colocalization Highlighter" plug-in in ImageJ 1.41e to highlight the colocalizing pixels as white pixels. Default settings were used for most of the cases.

Alignment Accuracy Estimates

We conducted a systematic analysis by testing images from 171 different larvae. Pearson's correlation coefficient was calculated for each aligned expression image with the corresponding gene-specific average.

Modeling *Platynereis* Brain Anatomy

Amira 4.1.1 was used to segment various anatomical structures in the brain (Movie S4) and to generate 3D surface renderings shown in Figure 5.

Ectopic Overexpression of Wnt Canonical Signaling

We used an established procedure (Schneider and Bowerman, 2007) of treatment with 1-Azakenpaullone (cat. no. 191500, Calbiochem) to achieve ectopic overexpression of canonical Wnt signaling in *Platynereis dumerilii* larvae. A mixture of larvae from two to three different animal pairs was used for treatment. The larvae were treated from 24 hpf to 48 hpf in 6 ml Natural Sea Water at a final concentration of 1 μM 1-Azakenpaullone or DMSO and were grown at 18°C. The larvae were fixed in 4% PFA/PTW, stored in 100% methanol at −20°C, and proceeded for in situ hybridization. The staining reactions were stopped simultaneously for control and treated larvae, much before the saturation.

Cloning Genes

We used degenerate primers to clone fragments of *brn1/2/4*, *dach*, *emx*, *svp*, *tll*, *vglut*, and *gad* and 5′,3′-RACE extensions to extend the fragments (see the Extended Experimental Procedures for primer sequences). We used cDNA templates generated with SMART technology (SMART RACE cDNA amplification kit, Clonetech) from total RNA extracted from larvae at several developmental stages. Other genes investigated in this study were obtained either as EST sequences or from previous publications. The GenBank IDs of *arx*, *ash2*, *bf-1*, *brn1/2/4*, *coe*, *dach*, *emx*, *er81*, *ets3*, *lhx1/5*, *svp*, *tll*, *vglut*, *Wnt5*, *Wnt8*, *gad*, and *tyr hyd* are GU169412–GU169428, respectively.

SUPPLEMENTAL INFORMATION

Supplemental Information includes Extended Experimental Procedures, five figures, and four movies and can be found with this article online at doi: 10.1016/j.cell.2010.07.043.

ACKNOWLEDGMENTS

We thank F. Christodoulou for providing larvae stained with mir-9, 9*, H. Snyman for expert technical assistance, and the Arendt lab for support. The electron micrograph in Figure 5 was taken with C. Nielsen during a practical course. R.T. and K.T.-R. were supported by fellowships of the Marie Curie RTN ZOONET (MRTN-CT-2004-005624), R.T. by DFG Collaborative Research Network SFB-488, and A.D. by a Louis Jeantet Foundation fellowship. R.T. conceived and developed PrImR, designed and performed the experiments, analyzed and interpreted the data, and wrote the paper. A.S.D. contributed clones of *vglut* and *gad*. K.T.-R. contributed clones of *brn124* and *emx*. D.A. proposed to study annelid mushroom bodies, provided ideas, interpreted the data, and wrote the paper.

Received: March 12, 2010
Revised: May 22, 2010
Accepted: July 14, 2010
Published: September 2, 2010

REFERENCES

Arendt, D. (2005). Genes and homology in nervous system evolution: comparing gene functions, expression patterns, and cell type molecular fingerprints. Theory Biosci. *24*, 185–197.

Arendt, D. (2008). The evolution of cell types in animals: emerging principles from molecular studies. Nat. Rev. Genet. *9*, 868–882.

Arendt, D., Tessmar, K., de Campos-Baptista, M.I., Dorresteijn, A., and Wittbrodt, J. (2002). Development of pigment-cup eyes in the polychaete Platynereis dumerilii and evolutionary conservation of larval eyes in Bilateria. Development *129*, 1143–1154.

Backman, M., Machon, O., Mygland, L., van den Bout, C.J., Zhong, W., Taketo, M.M., and Krauss, S. (2005). Effects of canonical Wnt signaling on dorso-ventral specification of the mouse telencephalon. Dev. Biol. *279*, 155–168.

Bani-Yaghoub, M., Tremblay, R.G., Lei, J.X., Zhang, D., Zurakowski, B., Sandhu, J.K., Smith, B., Ribecco-Lutkiewicz, M., Kennedy, J., Walker, P.R., and Sikorska, M. (2006). Role of Sox2 in the development of the mouse neocortex. Dev. Biol. *295*, 52–66.

Caubit, X., Thangarajah, R., Theil, T., Wirth, J., Nothwang, H.G., Rüther, U., and Krauss, S. (1999). Mouse Dac, a novel nuclear factor with homology to Drosophila dachshund shows a dynamic expression in the neural crest, the eye, the neocortex, and the limb bud. Dev. Dyn. *214*, 66–80.

Christodoulou, F., Raible, F., Tomer, R., Simakov, O., Trachana, K., Klaus, S., Snyman, H., Hannon, G.J., Bork, P., and Arendt, D. (2010). Ancient animal microRNAs and the evolution of tissue identity. Nature *463*, 1084–1088.

Danesin, C., Peres, J.N., Johansson, M., Snowden, V., Cording, A., Papalopulu, N., and Houart, C. (2009). Integration of telencephalic Wnt and hedgehog signaling center activities by Foxg1. Dev. Cell *16*, 576–587.

Denes, A.S., Jékely, G., Steinmetz, P.R., Raible, F., Snyman, H., Prud'homme, B., Ferrier, D.E., Balavoine, G., and Arendt, D. (2007). Molecular architecture of annelid nerve cord supports common origin of nervous system centralization in bilateria. Cell *129*, 277–288.

Deo, M., Yu, J.Y., Chung, K.H., Tippens, M., and Turner, D.L. (2006). Detection of mammalian microRNA expression by in situ hybridization with RNA oligonucleotides. Dev. Dyn. *235*, 2538–2548.

Ekonomou, A., Kazanis, I., Malas, S., Wood, H., Alifragis, P., Denaxa, M., Karagogeos, D., Constanti, A., Lovell-Badge, R., and Episkopou, V. (2005). Neuronal migration and ventral subtype identity in the telencephalon depend on SOX1. PLoS Biol. *3*, e186.

Evans, S.M. (1966). Non-associative behavioural modifications in nereid polychaetes. Nature *211*, 945–948.

Farris, S.M. (2005). Evolution of insect mushroom bodies: old clues, new insights. Arthropod Struct. Dev. *34*, 211–234.

Farris, S.M. (2008). Evolutionary convergence of higher brain centers spanning the protostome-deuterostome boundary. Brain Behav. Evol. *72*, 106–122.

Fischer, A., and Dorresteijn, A.W.C. (2004). The polychaete Platynereis dumerilii (Annelida): a laboratory animal with spiralian cleavage, lifelong segment proliferation and a mixed benthic/pelagic life cycle. Bioessays *26*, 314–325.

Förster, E., Zhao, S., and Frotscher, M. (2006). Laminating the hippocampus. Nat. Rev. Neurosci. *7*, 259–267.

Garel, S., Marín, F., Grosschedl, R., and Charnay, P. (1999). Ebf1 controls early cell differentiation in the embryonic striatum. Development *126*, 5285–5294.

Hébert, J.M., and Fishell, G. (2008). The genetics of early telencephalon patterning: some assembly required. Nat. Rev. Neurosci. *9*, 678–685.

Heisenberg, M. (2003). Mushroom body memoir: from maps to models. Nat. Rev. Neurosci. *4*, 266–275.

Houart, C., Caneparo, L., Heisenberg, C., Barth, K., Take-Uchi, M., and Wilson, S. (2002). Establishment of the telencephalon during gastrulation by local antagonism of Wnt signaling. Neuron *35*, 255–265.

Inoue, T., Nakamura, S., and Osumi, N. (2000). Fate mapping of the mouse prosencephalic neural plate. Dev. Biol. *219*, 373–383.

Jékely, G., and Arendt, D. (2007). Cellular resolution expression profiling using confocal detection of NBT/BCIP precipitate by reflection microscopy. Biotechniques *42*, 751–755.

Kandel, E.R.S., James, H., and Jessell, T.M. (2000). Principles of Neural Science, Fourth Edition (New York: McGraw-Hill Companies, Inc.).

Keeble, T.R., Halford, M.M., Seaman, C., Kee, N., Macheda, M., Anderson, R.B., Stacker, S.A., and Cooper, H.M. (2006). The Wnt receptor Ryk is required for Wnt5a-mediated axon guidance on the contralateral side of the corpus callosum. J. Neurosci. *26*, 5840–5848.

Kimura, J., Suda, Y., Kurokawa, D., Hossain, Z.M., Nakamura, M., Takahashi, M., Hara, A., and Aizawa, S. (2005). Emx2 and Pax6 function in cooperation with Otx2 and Otx1 to develop caudal forebrain primordium that includes future archipallium. J. Neurosci. *25*, 5097–5108.

Liu, X., Long, F., Peng, H., Aerni, S.J., Jiang, M., Sánchez-Blanco, A., Murray, J.I., Preston, E., Mericle, B., Batzoglou, S., et al. (2009). Analysis of cell fate from single-cell gene expression profiles in C. elegans. Cell *139*, 623–633.

Marín, O., and Rubenstein, J.L. (2001). A long, remarkable journey: tangential migration in the telencephalon. Nat. Rev. Neurosci. *2*, 780–790.

McEvilly, R.J., de Diaz, M.O., Schonemann, M.D., Hooshmand, F., and Rosenfeld, M.G. (2002). Transcriptional regulation of cortical neuron migration by POU domain factors. Science *295*, 1528–1532.

Miura, H., Yanazawa, M., Kato, K., and Kitamura, K. (1997). Expression of a novel aristaless related homeobox gene 'Arx' in the vertebrate telencephalon, diencephalon and floor plate. Mech. Dev. *65*, 99–109.

Müller, W.A. (1973). [Autoradiographic studies on the synthetic activity of neurosecretory cells in the brain of Platynereis dumerilii during sexual development and regeneration]. Z. Zellforsch. Mikrosk. Anat. *139*, 487–510.

Nieto, M., Schuurmans, C., Britz, O., and Guillemot, F. (2001). Neural bHLH genes control the neuronal versus glial fate decision in cortical progenitors. Neuron *29*, 401–413.

Nieuwenhuys, R. (2002). Deuterostome brains: synopsis and commentary. Brain Res. Bull. *57*, 257–270.

Noveen, A., Daniel, A., and Hartenstein, V. (2000). Early development of the Drosophila mushroom body: the roles of eyeless and dachshund. Development *127*, 3475–3488.

Raible, F., Tessmar-Raible, K., Osoegawa, K., Wincker, P., Jubin, C., Balavoine, G., Ferrier, D.E., Benes, V., de Jong, P., Weissenbach, J., et al. (2005). Vertebrate-type intron-rich genes in the marine annelid *Platynereis dumerilii*. Science *310*, 1325–1326.

Schneider, S.Q., and Bowerman, B. (2007). beta-Catenin asymmetries after all animal/vegetal- oriented cell divisions in Platynereis dumerilii embryos mediate binary cell-fate specification. Dev. Cell *13*, 73–86.

Shimamura, K., Hartigan, D.J., Martinez, S., Puelles, L., and Rubenstein, J.L. (1995). Longitudinal organization of the anterior neural plate and neural tube. Development *121*, 3923–3933.

Stigloher, C., Ninkovic, J., Laplante, M., Geling, A., Tannhäuser, B., Topp, S., Kikuta, H., Becker, T.S., Houart, C., and Bally-Cuif, L. (2006). Segregation of telencephalic and eye-field identities inside the zebrafish forebrain territory is controlled by Rx3. Development *133*, 2925–2935.

Strausfeld, N.J., and Barth, F.G. (1993). Two visual systems in one brain: neuropils serving the secondary eyes of the spider Cupiennius salei. J. Comp. Neurol. *328*, 43–62.

Strausfeld, N.J., Hansen, L., Li, Y., Gomez, R.S., and Ito, K. (1998). Evolution, discovery, and interpretations of arthropod mushroom bodies. Learn. Mem. *5*, 11–37.

Strausfeld, N.J., Strausfeld, C.M., Loesel, R., Rowell, D., and Stowe, S. (2006). Arthropod phylogeny: onychophoran brain organization suggests an archaic relationship with a chelicerate stem lineage. Proc Biol Sci *273*, 1857–1866.

Strausfeld, N.J., Sinakevitch, I., Brown, S.M., and Farris, S.M. (2009). Ground plan of the insect mushroom body: functional and evolutionary implications. J. Comp. Neurol. *513*, 265–291.

Sugino, K., Hempel, C.M., Miller, M.N., Hattox, A.M., Shapiro, P., Wu, C., Huang, Z.J., and Nelson, S.B. (2006). Molecular taxonomy of major neuronal classes in the adult mouse forebrain. Nat. Neurosci. *9*, 99–107.

Swanson, L.W. (2000). Cerebral hemisphere regulation of motivated behavior. Brain Res. *886*, 113–164.

Taglialatela, P., Soria, J.M., Caironi, V., Moiana, A., and Bertuzzi, S. (2004). Compromised generation of GABAergic interneurons in the brains of Vax1-/- mice. Development *131*, 4239–4249.

Tessmar-Raible, K., Steinmetz, P.R.H., Snyman, H., Hassel, M., and Arendt, D. (2005). Fluorescent two-color whole mount in situ hybridization in Platynereis dumerilii (Polychaeta, Annelida), an emerging marine molecular model for evolution and development. Biotechniques *39*, 460, 462, 464.

Tessmar-Raible, K., Raible, F., Christodoulou, F., Guy, K., Rembold, M., Hausen, H., and Arendt, D. (2007). Conserved sensory-neurosecretory cell types in annelid and fish forebrain: insights into hypothalamus evolution. Cell *129*, 1389–1400.

Tole, S., Ragsdale, C.W., and Grove, E.A. (2000). Dorsoventral patterning of the telencephalon is disrupted in the mouse mutant extra-toes(J). Dev. Biol. *217*, 254–265.

Tuoc, T.C., and Stoykova, A. (2008). Er81 is a downstream target of Pax6 in cortical progenitors. BMC Dev. Biol. *8*, 23.

Urbach, R., and Technau, G.M. (2003). Molecular markers for identified neuroblasts in the developing brain of Drosophila. Development *130*, 3621–3637.

Viola, P.A., and Wells, W.M., III. (1995). Alignment by maximization of mutual information. International Journal of Computer Vision *24*, 137–154.

Wang, B., Waclaw, R.R., Allen, Z.J., 2nd, Guillemot, F., and Campbell, K. (2009). Ascl1 is a required downstream effector of Gsx gene function in the embryonic mouse telencephalon. Neural Dev *4*, 5.

Woodger, J.H. (1945). On biological transformations. In Essays on Growth and Form, presented to D'Arcy Wentworth Thompson, W.E. le Gros Clark and P.B. Medawar, eds. (Oxford: Oxford University Press), pp. 95–120.

Yun, K., Potter, S., and Rubenstein, J.L. (2001). Gsh2 and Pax6 play complementary roles in dorsoventral patterning of the mammalian telencephalon. Development *128*, 193–205.